On Hybrid Pressure Broadening Studies

J. Singh, P.A.M. Dolph, V.V. Nelyubin, W.A. Tobias, G.D. Cates,
and some WM people?
University of Virginia
Version 0.50

May 1, 2006

Abstract

It is proposed that precision pressure broadening measurements be made on the D1 and D2 lines of Potassium and Rubidium in the presence of ^{3}He and N_2 buffer gases as a function of temperature. These data will be needed to determine the ^{3}He at the percent level. As far as we know, there do not exist high pressure data for Potassium. In addition, the temperature dependance of the broadening is poorly understood at temperatures above 100 C. As a bonus, one also gets the alkali densities and vapor ratio "for free" as a consequence of the data analysis. This information can be used as a rough gauge of both (1) how well we can prepare a prescribed ratio of [K]:[Rb] and (2) the ^{3}He polarization performance as a function of akali density ratio. Preliminary results of all the cells characterized for G_E^n will be presented, including polarization performance vs. density ratio.

Contents

1 "Online" Analysis

1.1 Raw Data (Ideal Case)

The Ti:Sapphire (aka Single Frequency aka Ring) laser has a frequency dependant intensity given by $I_0(\nu)$. The intensity transmitted through the PB oven and cell is given by:

$$I_t(\nu) = I_0(\nu) \exp\left(-[A]\sigma(\nu)l\right) \tag{1}$$

where $[A]$ is the number density of the alkali vapor, σ is the absorption cross section per unit frequency, and l is the path length through the cell. The reference and transmitted intensities are converted into AC voltages (due to the chopper) by the photodiodes, amplified by the "photodiode box," converted into DC signals by the lock-ins, and finally digitized by the "autoscan interface box:"

$$N_{\text{ref}}(\nu) = G_{\text{PD1}} G_{\text{PD1-box}} G_{\text{lockin-1}} G_{\text{ADC}} I_0(\nu) \tag{2}$$

$$N_{\text{trans}}(\nu) = G_{\text{PD2}} G_{\text{PD2-box}} G_{\text{lockin-2}} G_{\text{ADC}} I_t(\nu) \tag{3}$$

where N is the number of bits from 0 to 4095 that the data channel reads. The raw data recorded in the ".SCN" file are the frequencies and the values of N_{ref} and N_{trans} in binary format. Before analysis, they have to be converted into ASCII format using a LabVIEW vi called "readscn.vi."

2 Quick Single Lorentzian Fit

We ultimately want to fit to $\sigma(\nu)$. Therefore the analysis program first makes the following transformation:

$$x = \nu \tag{4}$$

$$y = \log\left(\frac{N_{\text{trans}}}{N_{\text{ref}}}\right) \tag{5}$$

$$= -[A]\sigma(\nu)l + \log\left(\frac{G_{\text{PD2}} G_{\text{PD2-box}} G_{\text{lockin-2}}}{G_{\text{PD1}} G_{\text{PD1-box}} G_{\text{lockin-1}}}\right) \tag{6}$$

The absorption cross section is given by a lorentzian with a small dispersion-like term:

$$\sigma(\nu) = \frac{\sigma_0}{\pi} \frac{\frac{\Gamma}{2}\left[1 + 0.664 \times 2\pi T_d \left(\nu - \nu_0\right)\right]}{\left(\nu - \nu_0\right)^2 + \frac{\Gamma^2}{4}} \tag{7}$$

$$\int_0^\infty \sigma(\nu) \mathrm{d}\nu = \sigma_0 = \pi r_e c f \tag{8}$$

Putting this altoghether gives:

$$y = -[A]l\frac{\sigma_0}{\pi} \frac{\frac{\Gamma}{2}\left[1 + 0.664 \times 2\pi T_d \left(\nu - \nu_0\right)\right]}{\left(\nu - \nu_0\right)^2 + \frac{\Gamma^2}{4}} + \log\left(\frac{G_{\text{PD2}} G_{\text{PD2-box}} G_{\text{lockin-2}}}{G_{\text{PD1}} G_{\text{PD1-box}} G_{\text{lockin-1}}}\right) \tag{9}$$

$$= \frac{c_0\left[1 + 0.664 \times 2\pi c_1 \left(x - c_2\right)\right]}{\left(x - c_2\right)^2 + \frac{c_3^2}{4}} + c_4 \tag{10}$$

$$c_0 = -\frac{[A]l\sigma_0\Gamma}{2\pi} \quad \left(\text{GHz}^2\right) \tag{11}$$

$$c_1 = T_d \quad \left(\text{GHz}^{-1}\right) \tag{12}$$

$$c_2 = \nu_0 \quad (\text{GHz}) \tag{13}$$

$$c_3 = \Gamma \quad (\text{GHz}) \tag{14}$$

$$c_4 = \log\left(\frac{G_{\text{PD2}} G_{\text{PD2-box}} G_{\text{lockin-2}}}{G_{\text{PD1}} G_{\text{PD1-box}} G_{\text{lockin-1}}}\right) \quad (\text{unitless}) \tag{15}$$

Equation (10) is fit to get the parameters c_0,c_1,c_2,c_3 and c_4.

2.1 ^{3}He Density

The density of the buffer gas is proportional to the FWHM (full-width half maximum) of the lineshape:

$$c_3 = \Gamma = \langle\sigma v\rangle_{\mathrm{Rb-{}^3He}}[^3\mathrm{He}] + \langle\sigma v\rangle_{\mathrm{Rb-N_2}}[\mathrm{N_2}] \tag{16}$$

$$\langle\sigma v\rangle_{\mathrm{Rb-D_1-{}^3He}} = 18.7\left(\frac{T}{353\ \mathrm{K}}\right)^{0.05}\ \frac{\mathrm{GHz}}{\mathrm{amagat}} \tag{17}$$

$$\langle\sigma v\rangle_{\mathrm{Rb-D_1-N_2}} = 17.8\left(\frac{T}{353\ \mathrm{K}}\right)^{0.30}\ \frac{\mathrm{GHz}}{\mathrm{amagat}} \tag{18}$$

$$\langle\sigma v\rangle_{\mathrm{Rb-D_2-{}^3He}} = 20.8\left(\frac{T}{353\ \mathrm{K}}\right)^{0.53}\ \frac{\mathrm{GHz}}{\mathrm{amagat}} \tag{19}$$

$$\langle\sigma v\rangle_{\mathrm{Rb-D_2-N_2}} = 18.1\left(\frac{T}{353\ \mathrm{K}}\right)^{0.30}\ \frac{\mathrm{GHz}}{\mathrm{amagat}} \tag{20}$$

To get the correct helium density, one has to know the temperature of the cell and the nitrogen density (gotten from filling data). (Reference: Romalis, Miron, and Cates, PRA Vol 56 Num 6 p4569 (1997))

2.2 Alkali Density

The alkali density is proportional to the size of the the "absorption dip" of the lineshape:

$$[A] = -c_0\frac{2\pi}{l\sigma_0\Gamma} \tag{21}$$

$$= -c_0\frac{2\pi}{l\pi r_e c f c_3} \tag{22}$$

$$= -\frac{c_0}{c_3}\frac{2}{l r_e c f} \tag{23}$$

where l is the path length through the cell, $r_e = 2.817940325\times10^{-15}$ m (classical electron radius), c is the speed of light, and f is the oscillator strength of the transition. For both rubidium and potassium, $f = 1/3$ for the D1 transition and $f = 2/3$ for the D2 transition.

In principle, one can also get the alkali density by integrating over the lineshape:

$$\int_{c_2-\Delta x}^{c_2+\Delta x} y(x)\ \mathrm{d}x = \int_{c_2-\Delta x}^{c_2+\Delta x} \frac{c_0}{(x-c_2)^2+\frac{c_3^2}{4}} + \frac{c_0 0.664\times 2\pi c_1\,(x-c_2)}{(x-c_2)^2+\frac{c_3^2}{4}} + c_4\ \mathrm{d}x \tag{24}$$

$$\lim_{\Delta x\to\infty}\int_{c_2-\Delta x}^{c_2+\Delta x} \frac{c_0}{(x-c_2)^2+\frac{c_3^2}{4}}\ \mathrm{d}x = 2\pi\frac{c_0}{c_3} \tag{25}$$

$$\int_{c_2-\Delta x}^{c_2+\Delta x} \frac{x-c_2}{(x-c_2)^2+\frac{c_3^2}{4}}\ \mathrm{d}x = 0\ \text{(by symmetry)} \tag{26}$$

$$\int_{c_2-\Delta x}^{c_2+\Delta x} c_4\ \mathrm{d}x = 2c_4\Delta x \tag{27}$$

where the alkali density is gotten from:

$$p \equiv \int_{c_2-\Delta x}^{c_2+\Delta x} y(x)\ \mathrm{d}x \tag{28}$$

$$\approx 2\pi\frac{c_0}{c_3} + 2c_4\Delta x \tag{29}$$

$$[A] \approx -\frac{(p-2c_4\Delta x)}{l\pi r_e c f} \tag{30}$$

To do this, one must be very certain that the background integrates to zero ($c_4 \approx 0$) or to some well known value.

2.3 Temperature Dependance of Magic Constant ($\langle\sigma v\rangle$)

It's important to make a few comments about the temperature dependance of these constants:

1. The temperature dependance was only measured for Rb-^{4}He broadening at 60 C, 80 C, and 100 C.
2. The temperature dependance of the magic constant ($\langle\sigma v\rangle$) was assumed to come solely from the relative velocity of the reduced mass system.
3. The fit to the temperature dependance of Rb-^{4}He includes data from Rb-^{3}He at 80 C scaled by the ratio of the relative velcities of these two systems:

$$\frac{1}{\mu_{\rm n}} = \frac{1}{m_{\rm Rb}} + \frac{1}{m_{^{\rm n}{\rm He}}} \tag{31}$$

$$\langle v_{\rm rel}\rangle = \sqrt{\frac{2RT}{\mu}} \tag{32}$$

$$\langle\sigma v\rangle_{{\rm Rb-D_x-}^4{\rm He}}\left(\text{ at } {\rm T_{eff}} = \frac{\mu_4}{\mu_3}{\rm T}\right) = \langle\sigma v\rangle_{{\rm Rb-D_x-}^3{\rm He}}(\text{ at T}) \tag{33}$$

4. A van der Waals potential was is assumed in order to calculate the first order correction to the pressure broadening lineshape (dispersion term in equation 7). A van der Waals potential also predicts a $T^{0.3}$ temperature dependance which was not observed for the Rb-He system.
5. The Rb-N_2 temperature dependance is assumed from theory because it is was not measured.

To get the temperature dependance from the data, ignoring the small contribution from the N_2, we can fit a line to a log-log plot:

$$c_3 = \Gamma \approx \langle\sigma v\rangle_T [^3{\rm He}] \tag{34}$$

$$\underbrace{\log c_3}_{y} = \underbrace{\log\left(\langle\sigma v\rangle_{80}[^3{\rm He}]\right)}_{b} + n\underbrace{\log\left(\frac{T}{353\text{ K}}\right)}_{x} \tag{35}$$

$$y = b + nx \tag{36}$$

where $\langle\sigma v\rangle_{80}$ is the magic constant at 80 C and b and n are free parameters.

2.4 Temperature Dependance of the Alkali Density (Vapor Pressure Curve)

The vapor pressure and density above liquid for a pure sample of an alkali metal is given by:

$$\log_{10}\left(\frac{p}{1\text{ atm}}\right) = A - \frac{B}{T} \tag{37}$$

$$\rho = [A] = \frac{p}{RT}\quad\left(\frac{\text{moles}}{\text{liter}}\right) \tag{38}$$

where R is the universal gas constant:

$$R = 0.08205746\ \frac{\text{liter}\cdot\text{atm}}{\text{moles}\cdot\text{K}} \tag{39}$$

For an impure sample, the vapor pressure is modified to approximately (Raoult's Law):

$$p = fp^0 \tag{40}$$

where f is the mole fraction of the alkali metal relative to everything in the sample and p^0 is the pure vapor pressure. The temperature dependance can be gotten from fitting to:

$$\underbrace{\log_{10}[A]}_{y} = \underbrace{(\log_{10} f + A - \log_{10} R)}_{b} - \underbrace{\log_{10} T}_{x_1} - \underbrace{\frac{B}{T}}_{x_2} \tag{41}$$

$$y = b - x_1 - Bx_2 \tag{42}$$

Element	A	B
Na	4.704	5377 K
K	4.402	4453 K
Rb	4.312	4040 K

Table 1: Vapor pressure coefficients (above liquid) for selected alkali metals from 1995 CRC

where b and B are free parameters. The temperature dependance of the K to Rb density ratio, $\mathcal{D}$, can be gotten from fitting to:

$$\log_{10}\ \mathcal{D} = \log_{10}\ \left(\frac{p_k/RT}{p_r/RT}\right) = \log_{10}\ \left(\frac{f_k p_k^0}{f_r p_r^0}\right) \tag{43}$$

$$\underbrace{\log_{10}\ \mathcal{D}}_{y} = \underbrace{\left(\log_{10}\frac{f_k}{f_r} + A_k - A_r\right)}_{b} - \underbrace{\overbrace{(B_k - B_r)}^{c}}_{x}\over{T} \tag{44}$$

$$y = b - cx \tag{45}$$

where b and c are free parameters and the subscripts k and r refer to Potassium and Rubidium respectively. For comparison, the "book" values for the A and B vapor pressure coefficients are listed in table 1.

2.5 Ratios of Magic Constants

Since there aleady exists a reliable number for the Rb magic constant at 80 C, if might prove convenient to cross calibrate with that measurement. This is done by taken the ratios of the line in question with Rb D1 or D2 line. For most measurements, it will be probably be better to look at ratios formed with the Rb D2 line because of increased SNR:

$$\frac{\Gamma_X}{\Gamma_{\mathrm{Rb-D2}}} = \frac{[^3\mathrm{He}]\,\langle\sigma v\rangle_{\mathrm{X}}(T)}{[^3\mathrm{He}]\,\langle\sigma v\rangle_{\mathrm{Rb-D2}}(T)} = \frac{\langle\sigma v\rangle_{\mathrm{X}}(T)}{\langle\sigma v\rangle_{\mathrm{Rb-D2}}(T)} \tag{46}$$

If we model the temperature dependance as a power law:

$$\frac{\Gamma_X}{\Gamma_{\mathrm{Rb-D2}}} = \frac{\langle\sigma v\rangle_{\mathrm{X}}(T)}{\langle\sigma v\rangle_{\mathrm{Rb-D2}}(T)} == \frac{\langle\sigma v\rangle_{\mathrm{X}}(353\mathrm{K})}{\langle\sigma v\rangle_{\mathrm{Rb-D2}}(353\mathrm{K})}\left(\frac{T}{353\mathrm{K}}\right)^{n_X - n_{\mathrm{Rb-D2}}} \tag{47}$$

Taking the log of sides gives

$$\log\frac{\Gamma_X}{\Gamma_{\mathrm{Rb-D2}}} = \log\left(\frac{\langle\sigma v\rangle_{\mathrm{X}}(353\mathrm{K})}{\langle\sigma v\rangle_{\mathrm{Rb-D2}}(353\mathrm{K})}\right) + (n_X - n_{\mathrm{Rb-D2}}) * \log\left(\frac{T}{353\mathrm{K}}\right) \tag{48}$$

$$y = A + Bx \tag{49}$$

which results in a linear form which is straightforward to fit.

2.6 Ratios of Alkali Densities

A useful way to charaterize the alkali density is to study it's deviation from the it's pure vapor pressure curve:

$$\log\frac{[A]L}{[A]_0} = (A - A_0)\log(10) + \log fL - \frac{B - B_0}{T}\log(10) \tag{50}$$

where f is the molar fraction of the alkali metal in the bulk form (solid or liquid depending on the temperature), $[A]$ is the number density of the alkali metal, A is the vapor pressure constant, B is the vapor pressure temperature coefficient, subcripts 0 refer to the pure vapor curve values (the "book" values), and L is the path length through the cell. The vapor pressure constants are atomic parameters that may be modified by

interactions with inpurities in bulk metal. If the bulk metal is relatively free of impurities and since Rb and K are chemically similar, it is not unreasonable to expect $A \approx A_0$ and $B \approx B_0$. Therefore most if not all of the temperature dependance should be removed. If L is known or can be estimated, then it can be divided out as well:

$$\log \frac{[A]}{[A]_0} = (A - A_0)\log(10) + \log f - \frac{B - B_0}{T}\log(10) \quad (51)$$

$$\log \frac{[A]}{[A]_0} \approx \log f - \frac{\Delta B}{T}\log(10) \quad (52)$$

where the expectation is that $\Delta B \approx 0$. Unfortunately, it is difficult to measure the path length precisely. However, ratios of alkali densities within the same cell are insensitive to the path length:

$$\log \frac{[A_2]L}{[A_1]L} = (A_2 - A_1)\log(10) + \log \frac{f_2}{f_1} - \frac{B_2 - B_1}{T}\log(10) \quad (53)$$

We can once again remove the pure vapor pressure curve contribution to this ratio:

$$\log \frac{[A_2]L[A_1]_0}{[A_1]L[A_2]_0} = (A_2 - A_2^0 - A_1 + A_1^0)\log(10) + \log \frac{f_2}{f_1} - \frac{B_2 - B_2^0 - B_1 + B_1^0}{T}\log(10) \quad (54)$$

Again the expectation is that $(A_2 - A_2^0 - A_1 + A_1^0) \approx 0)$ and $(B_2 - B_2^0 - B_1 + B_1^0) = \Delta\delta B \approx 0$:

$$\log \frac{[A_2]L[A_1]_0}{[A_1]L[A_2]_0} \approx \log \frac{f_2}{f_1} - \frac{\Delta\delta B}{T}\log(10) \quad (55)$$

In the above equations we've intentionally left a small temperature dependance. This will allow us to the gauge the necessity of the these terms by studying the results of the fit.

3 Preliminary Results

All the following data was obtained from quick online fits to a single lorentzian function. Therefore the data should be treated as good to $5 - 10\%$. For now, all uncertainties are scaled such that the reduced chi square is forced to 1. When appropriate, the data are wieghted by the SNR of the absorption lineshape. A more careful offline analysis is underway...

3.1 Magic Contants

Ratios of magic constants were obainted for each cell at each temperature. The noisest lowest temperature data was thrown out when necessary. The ratios were then averaged for each temperature with weights given by the sum of SNRs of data used to form the ratio. A line is fit to the log-log plot of the data for each combination of K and Rb lines in Figs (1)–(5). The data are consistent, however they do have large $\approx 6\%$ uncertainties. The uncertainties in the temperature dependances themselves are quite large for all the data.

3.2 Alkali Densities

There is a systematic difference between the alkali densities obtained from the D2 and D1 lines. An average was taken of the two by weighting the D2 twice as much as the D1. First the pure vapor pressure curve was divided out and then the "nominal" path length was divided out for each cell. A large pumping chamber cell was taken to have an inner diameter of 8.29 cm and the small pumping chamber cell was taken to gave an inner diameter of 5.75 cm. At this step we are sensitive to variations in cell geometries and that will be corrected for in the offline analysis. Finally the log of the data is fit to a line in Figs. (6)–(8).

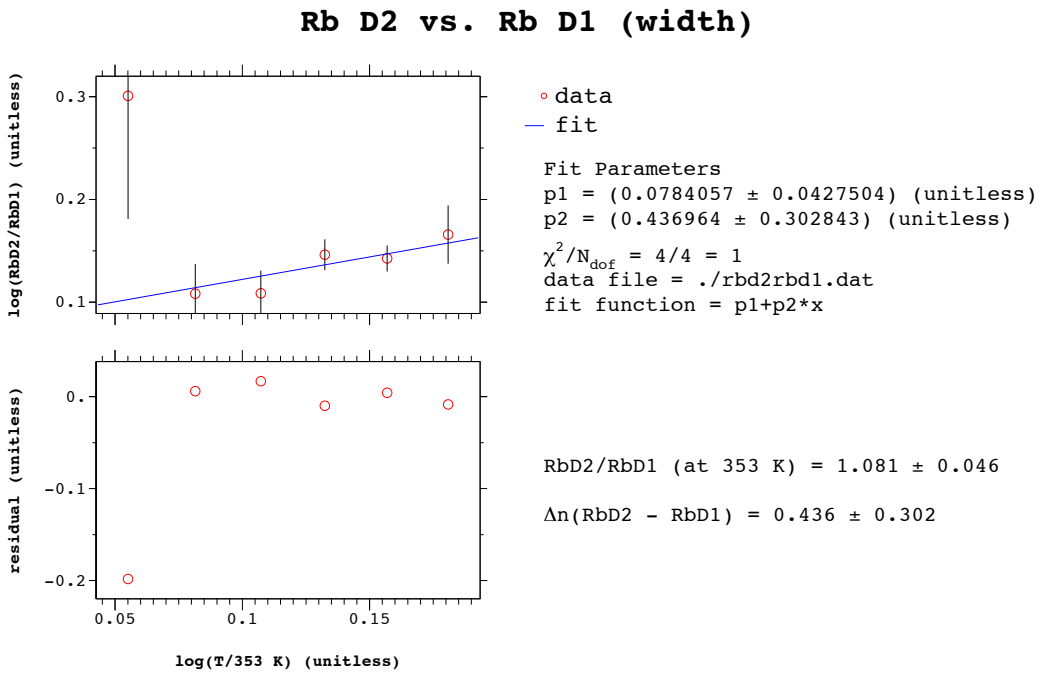

Figure 1: Rb D2 vs. Rb D1 as a function of temperature. Compare to Romalis et al: 0.48 ± 0.07 (temperature dependance difference) and ratio at 353 K of 1.112 ± 0.021.

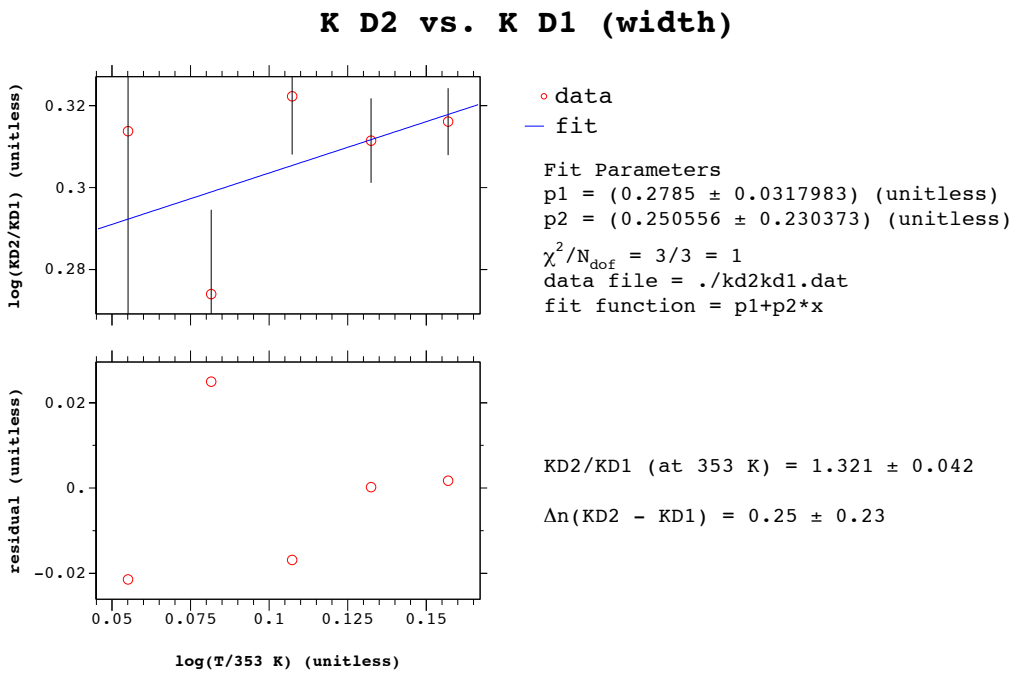

Figure 2: K D2 vs. K D1 as a function of temperature. This behaviour is quite different than for Rb.

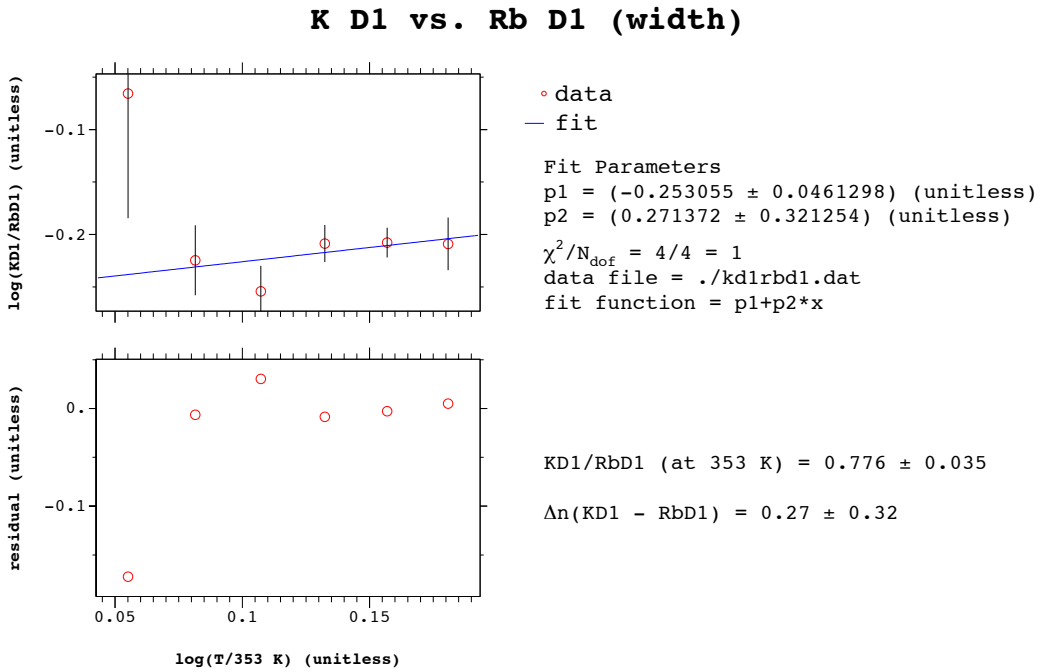

Figure 3: K D1 vs. Rb D1 as a function of temperature. Using Romalis et al.'s numbers, this gives $(14.5 \pm 0.5)\,(T/353\mathrm{K})^{0.32\pm0.32}$ for K D1.

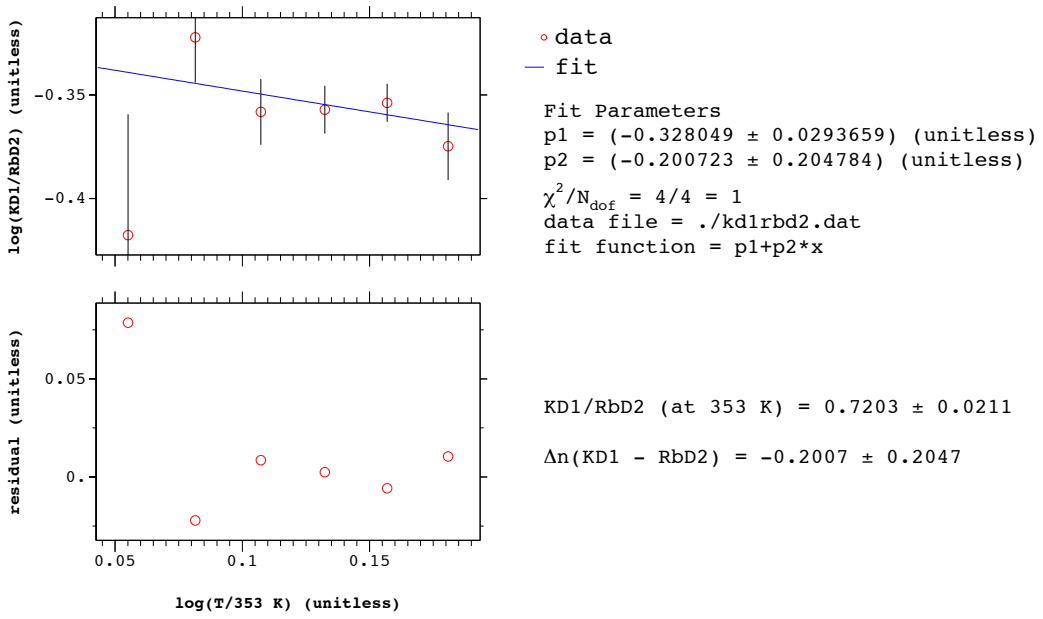

Figure 4: K D1 vs. Rb D2 as a function of temperature. Using Romalis et al.'s numbers, this gives $(15.0 \pm 0.5)\,(T/353\mathrm{K})^{0.33\pm0.21}$ for K D1.

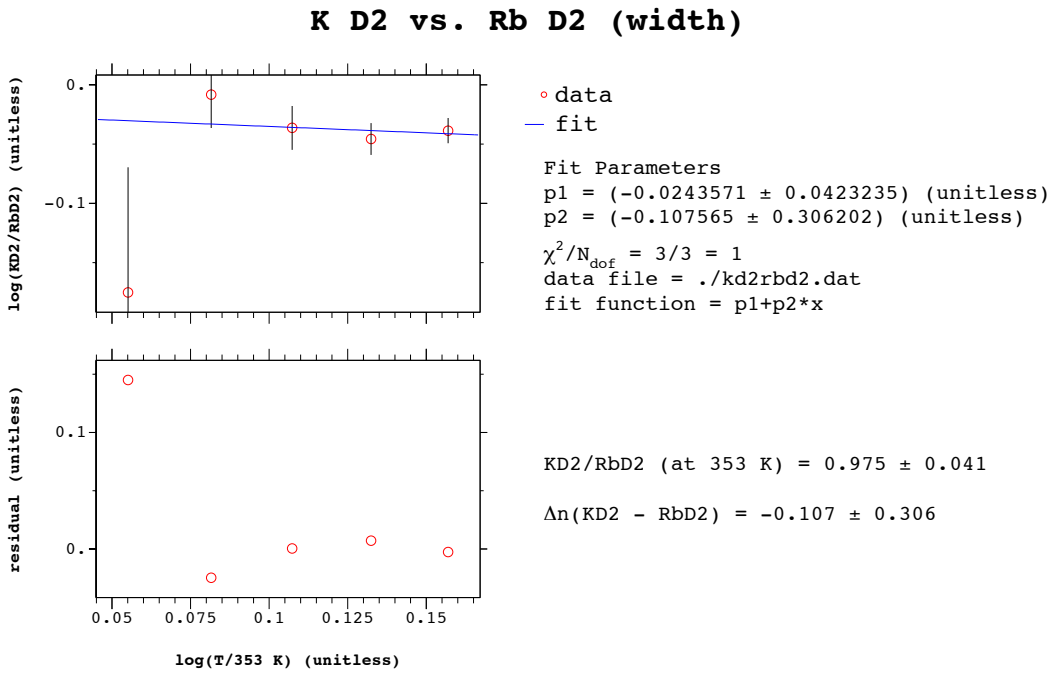

Figure 5: K D2 vs. Rb D2 as a function of temperature. Using Romalis et al.'s numbers, this gives $(20.3 \pm 0.9)\,(T/353\text{K})^{0.42\pm0.31}$ for K D2.

3.3 Performance vs. Ratio

Interpreting the performance data is complicated by fact that the polarization measurements were made with different light intensities, plus all of the other stuff...For Fig (9), this is handled by distinguishing the points by pumping chamber size (open and closed for small and LARGE) and total nominal power used (blue for 60W and less and red for 75W and more). Note that f_K and $f_R b$ are the molar fractions of K and Rb respectively in the bulk metal that sits in the cell. The sum of f_K and $f_R b$ gives some measure of the level of non-alkali metal impurities in the bulk metal. The bottom two plots show the density ratio vs. performance. The ratio is calculated using two methods, but they only differ significantly for Simone.

The final set of plots in Fig (10) our present best empirical guess of how the performance of hybrid cells varies as light intensity and density ratio. For the top two plots, the data points which represent a cell with a density ratio of less than 8 to 1 K:Rb at about 235 C are highlighted in red. We've seen that some cells do benefit from added laser power, but other do not. Particularly striking was Dolly. At the lower light intensities, it performed just as well as the other cells. However, when the intensity was roughly doubled, the performance did not improve much, if at all. It's possible that this is correlated with the fact that, of all the cell characterized for G_E^n, Dolly appears to have the largest K to Rb ratio, or equivalently the smallest amount of Rb. One possible explanation for this may be due to insufficient spin exchange between the K and Rb. Normally spin exchange between alkali atoms is very efficient. However, if there is not enough Rb to keep the K polarized, then a small polarization imbalance between the Rb and K can develop. When this happens, the small imbalance in alkali polarizations appears to the Rb as a large relaxation mechanism. This drives the average alkali polarization down.

The bottom plots in Fig (10) are the most intriguing. Here the red color highlights those measurements that were taken when the light intensity was very high. The argument for these red points is that the light intensity was so high that these measurements are relatively insensistive to the light intensity. If this is truly the case, the the difference is performance may then be most directly attributable to the density ratio. Concentrating on only the red points in the bottom right plot, one can image seeing a correlation between density ratio and performance.

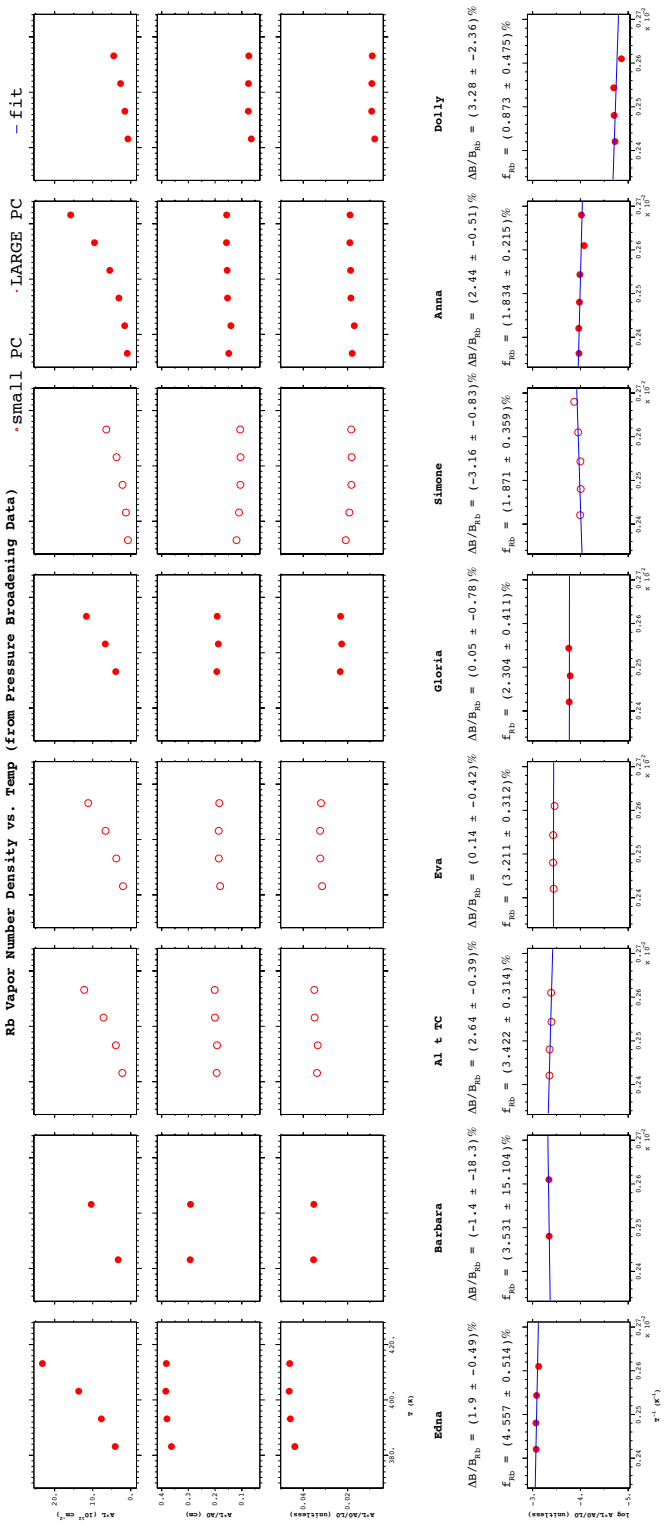

Figure 6: Rb Number Density vs. Temperature. Each column is cell. First row is the raw data. Second row is normalized to the pure vapor pressure curve. Third row is normalized to the nominal path length. The bottom row is the log-log fit. The residual temperature dependance is quite small for all the cells.

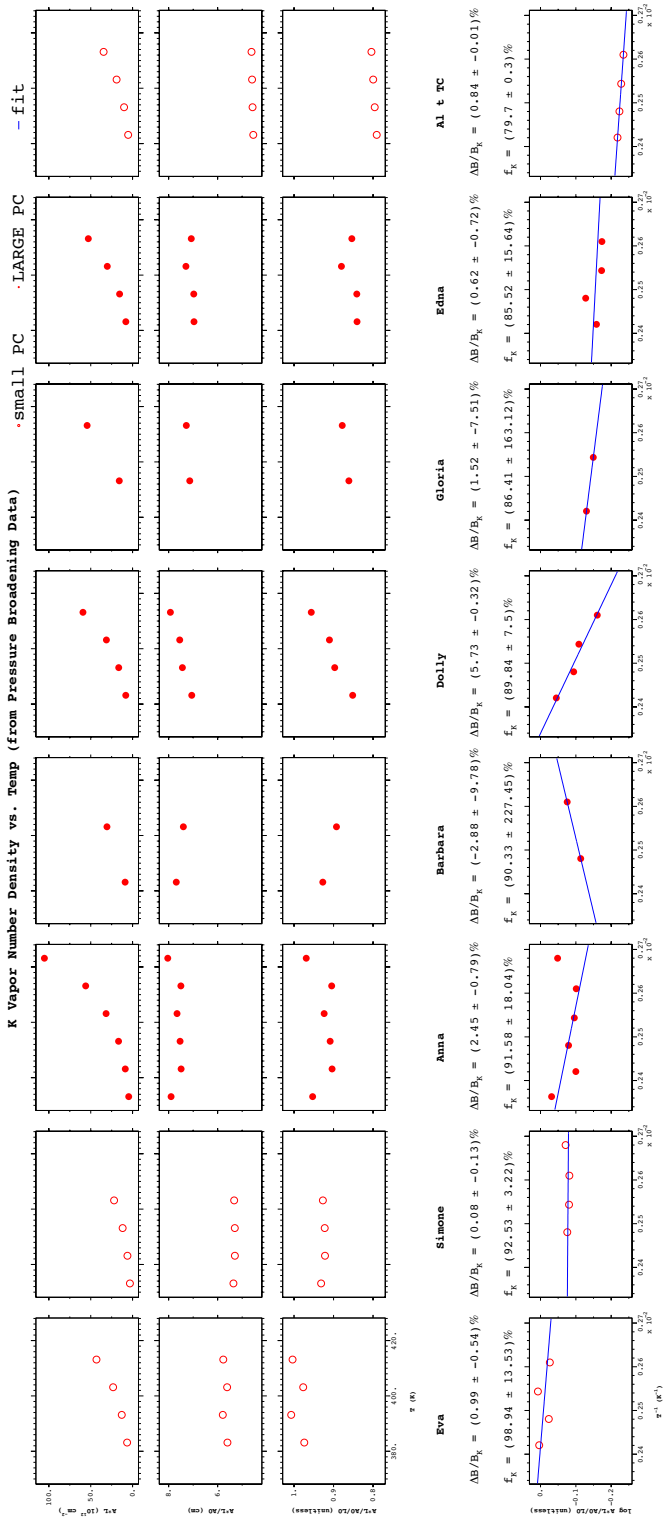

Figure 7: K Number Density vs. Temperature. Each column is cell. First row is the raw data. Second row is normalized to the pure vapor pressure curve. Third row is normalized to the nominal path length. The bottom row is the log-log fit. The residual temperature for K is larger than it was for Rb. Note however the vapor densities are all nearly 90% of what is expected from the pure vapor pressure curve.

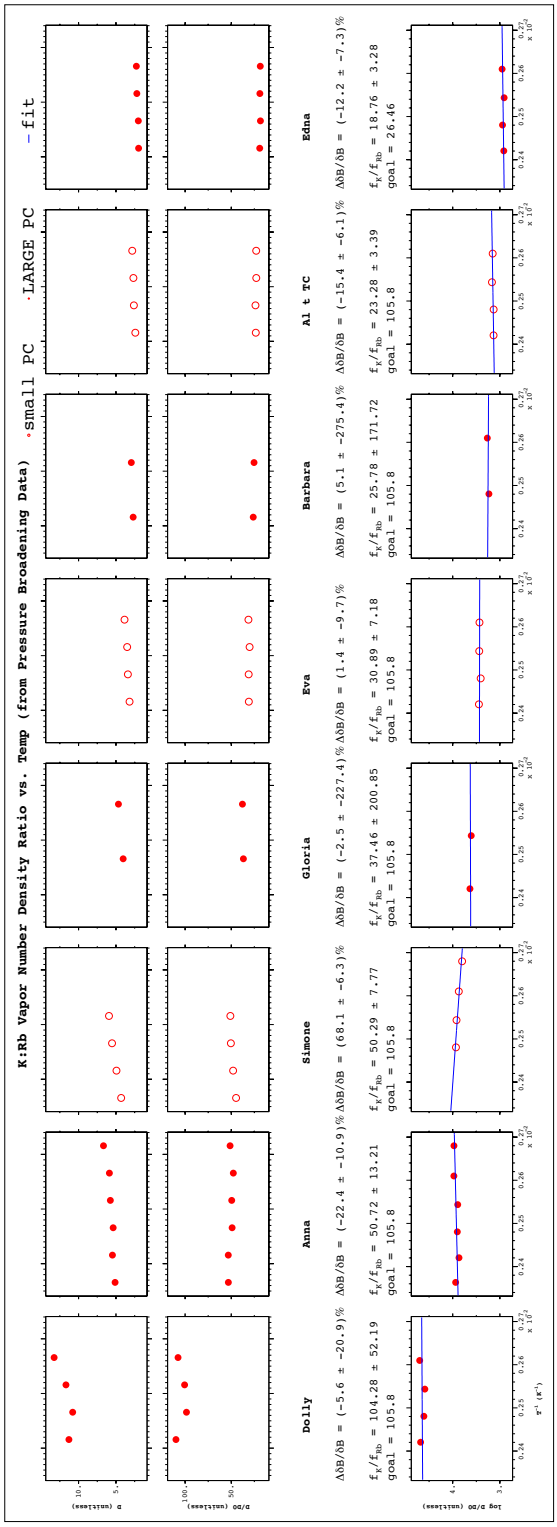

Figure 8: K:Rb Density Ratio vs. Temperature. Each column is cell. First row is the raw data. Second row is normalized to the pure vapor pressure curve. The bottom row is the log-log fit. The residual temperature dependance is generally quite small except for Simone. Note that there was about 8% variation in the Rb mole fraction during the ampuole preparation. However, this data implies about a 40% variation in the Rb mole fraction.

The star points are an extrapolation from low intensity measurements taken with Anna. The extrapolation was done to get a rough idea of how Anna might perform with more intensity. Note however that this is not a substitute for a direct measurement.

4 "Offline" Analysis

4.1 Introduction

Equation 10 is a good *first* pass fitting function. However, it neglects:

1. An oscillatory background due to imperfect cancellation of the interference pattern produced by the cover of the photodiodes.
2. Doppler broadening
3. Finite hyperfine splittings of the ground and excited states.
4. Natural isotopic composition of the alkali vapor
5. Possible "leakage" of the wings of nearby absorption lines

Note that we claim that the PB method is accurate at the 1 percent level (or even less); therefore we'll discuss the above points more carefully.

When trying to determine how small of an effect is small enough to ignore, it's important to keep in mind the relative scales of the lineshape. The FWHM of the absorption curve is about 20 GHz/amagat; so, an 8 amagat cell has about a 160 GHz FWHM. The frequency resolution (frequency jitter/noise and linewitdh) of the Ti:Sapphire is about 1 MHz. Data is acquired in about 1 GHz intervals. The accuracy of the Autoscan Wavemeter is in principle easily sub-GHz. However, in practice, the frequency can be shifted by as much as 20 GHz with the shift being independant of frequency. The quantities of interest are *insensitive* to the absolute frequency. This is because we only use the width of the line (and not the shift of the line) to determine the noble gas density. In addition, the alkali density is derived from the "size" of the dip and not from the "location." As a final note, it's important to mention that the data acquisition time interval and lock-in time constant are chosen carefully to minimize lock-in time averaging signal shaping effects (minimum time between points > five lock-in time constants).

4.2 Oscillatory Background

From past work (with JR), we know that the oscillations in the background come form the interference patterns that form due to the cover of the photodiodes. Both the transmitted and reference photodiodes have these patterns (Demtröder, Laser Spectroscopy, Enlarged 2nd Edition (1998), page 135, eq 4.51b):

$$I_{\text{trans}}(\nu) = I_0(\nu) \overbrace{\left[\frac{1}{1+F_t \sin^2\left(\frac{2\pi\nu n_t d_t \cos\theta_t}{c}\right)}\right]}^{\text{from Demtroder}} \exp\left(-[A]\sigma(\nu)l\right) \tag{56}$$

$$I_{\text{ref}}(\nu) = I_0(\nu) \left[\frac{1}{1+F_r \sin^2\left(\frac{2\pi\nu n_r d_r \cos\theta_r}{c}\right)}\right] \tag{57}$$

where F is an optical factor (see below) that encodes information about the reflectivity of the photodiode cover, n is the index of refraction of the cover, d is the thickness of the cover, θ is the angle of incidence, and the subscripts t and r refer to the transmitted and reference beams. Taking the log of the ratio:

$$y' = \log\left(\frac{I_{\text{trans}}}{I_{\text{ref}}}\right) \tag{58}$$

$$= \underbrace{-[A]\sigma(\nu)l + \log\left(\frac{G_t}{G_r}\right)}_{y} + \underbrace{\log\left[\frac{1+F_r \sin^2\left(\frac{2\pi\nu n_r d_r \cos\theta_r}{c}\right)}{1+F_t \sin^2\left(\frac{2\pi\nu n_t d_t \cos\theta_t}{c}\right)}\right]}_{q} \tag{59}$$

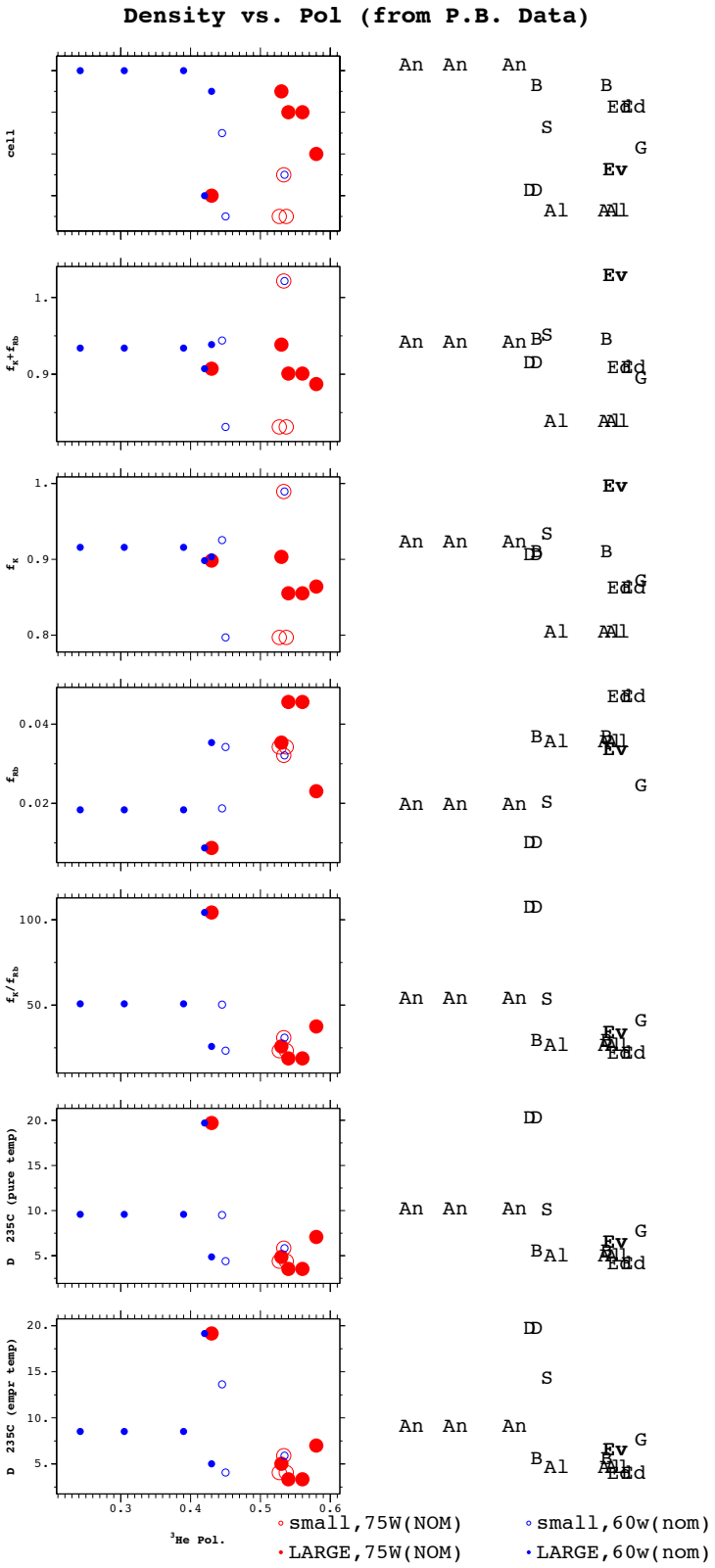

Figure 9: Various Parameters vs. Performance. Red is at least 75W. Blue is at most 60W. Closed circles are LARGE PC cells. Open circles are small PC cells.

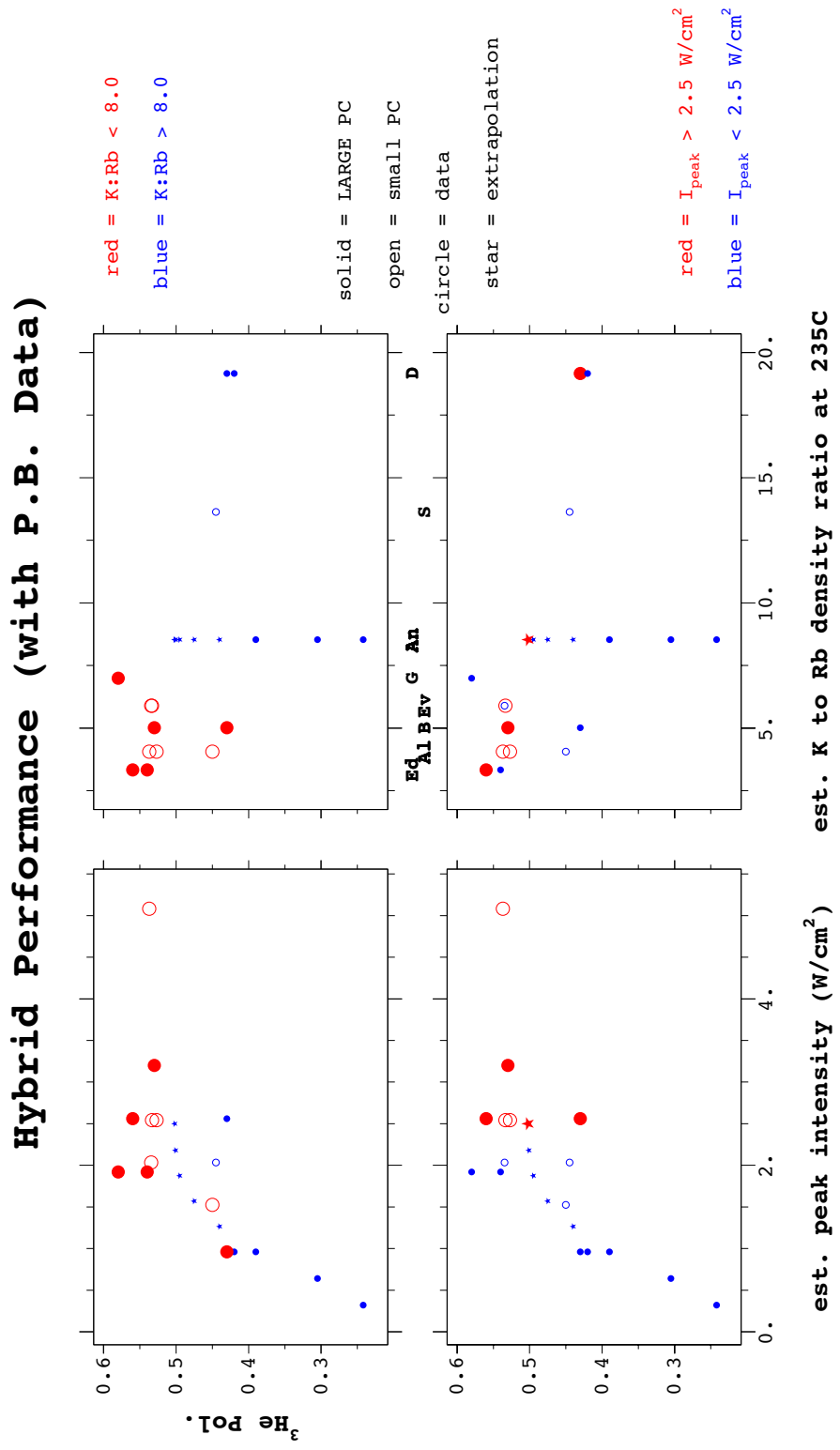

Figure 10: The Punchline. In the top plots, the red points are all cells with K:Rb ratios below 8.0. In the bottom plots, the red points are alls measurements taken with light intensities of at least 2.5 W/cm^2. Note that the star points are an extrapolation from lower intensity data for Anna.

F is calculated by the following (assuming interference from a parallel plate at normal incidence), where R is the reflectivity (*ibid*, page 153, eq 4.82):

$$F = \frac{4R}{(1-R)^2} \tag{60}$$

$$R = \left(\frac{n_1 - n_2}{n_1 + n_2}\right)^2 \tag{61}$$

where $n_{1,2}$ are the indices of refraction of the two materials. In our case, $n_1 \approx 1$ for air and $n_2 \approx 1.5$ for the glass/plastic cover, which gives $R \approx 0.04$ and $F \approx 0.16$. Since $F < 1$, we'll use the following first order expansion:

$$q = \log\left[\frac{1+\delta_1}{1+\delta_2}\right] \tag{62}$$

$$\approx \log\left[1 + \delta_1 - \delta_2\right] \tag{63}$$

$$\approx \delta_1 - \delta_2 \tag{64}$$

$$\approx F_r \sin^2\left(\frac{2\pi\nu n_r d_r \cos\theta_r}{c}\right) - F_t \sin^2\left(\frac{2\pi\nu n_t d_t \cos\theta_t}{c}\right) \tag{65}$$

$$\approx \frac{F_r}{2}\left[1 - \cos\left(\frac{4\pi\nu n_r d_r \cos\theta_r}{c}\right)\right] - \frac{F_t}{2}\left[1 - \cos\left(\frac{4\pi\nu n_t d_t \cos\theta_t}{c}\right)\right] \tag{66}$$

Note that if $F_r = F_t$ and $d_r \cos\theta_r = d_t \cos\theta_t$, then the interference terms cancel exactly. However the cancellation is very sensitive to the angles of incidence on the photodiode. In practice, the angles of incidence can be varied until the cancellation is optimal. If there are any residual oscillations, then they can be fit out using the following modified fit equation (ignoring higher order terms in $F_{r,t}$):

$$y' = y + q \tag{67}$$

$$y' = y + \frac{F_r}{2}\left[1 - \cos\left(\frac{4\pi\nu n_r d_r \cos\theta_r}{c}\right)\right] - \frac{F_t}{2}\left[1 - \cos\left(\frac{4\pi\nu n_t d_t \cos\theta_t}{c}\right)\right] \tag{68}$$

$$= (y - c_4) + c_4' - c_5 \cos\left(c_6\nu\right) + c_7 \cos\left(c_8\nu\right) \tag{69}$$

where y is the part of the fitting function that encodes information about the absorption. We've introduced four new parameters to account for the background oscillations:

$$c_4' = c_4 + \frac{F_r - F_t}{2} \quad \text{(unitless)} \tag{70}$$

$$c_5 = \frac{F_r}{2} \quad \text{(unitless)} \tag{71}$$

$$c_6 = \frac{4\pi n_r d_r \cos\theta_r}{c} \quad \left(\text{GHz}^{-1}\right) \tag{72}$$

$$c_7 = \frac{F_t}{2} \quad \text{(unitless)} \tag{73}$$

$$c_8 = \frac{4\pi n_t d_t \cos\theta_t}{c} \quad \left(\text{GHz}^{-1}\right) \tag{74}$$

4.3 Doppler Broadening

Doppler broadening of a spectral line is due to the Doppler shift. The Doppler width is obtained from the width of the velocity distribution of the gas molecules or atoms. In our case, this is the Maxwell velocity distribution, which is Gaussian. The FWHM as a fraction of the transition frequency is given by the formula (*ibid*, page 68, eq 3.43c):

$$\frac{\delta\nu_D}{\nu_0} = 7.16 \times 10^{-7} \sqrt{\frac{T \text{ (in Kelvin)}}{M \text{ (in grams per mole)}}} \tag{75}$$

For the D2 lines of Potassium and Rubidium at 150 C, the doppler widths are 0.91 GHz and 0.60 GHz respectively. These widths are less than one percent of the pressure broadened widths and are therefore negligible(?). For much lower pressure broadened widths, this is not negligible and the data must be fit to a Voigt profile, which is a convolution of a lorentzian lineshape (pressure broadening) with a gaussian lineshape (Doppler broadening). An alternative is to simulate the effect and determine a Doppler correction factor.

4.4 Finite Hyperfine Splitting, Isotopic Composition, and Wing Leakage

Table 2 lists the hyperfine splittings of all the alkali metal isotopes (AIV_{77} = Arimondo et al, RMP, 49, p31-75 (1977)). The natural abundance of each of these isotopes is listed in table 3 (NIST_{x} = NIST websites). The hyperfine interaction between the nuclear spin and electron angular momentum causes an additional small splitting of the spectral line. This splitting, if not accounted for, would appear as a slight additional broadening. All the excited state hyperfine splittings are less that 0.5 GHz and therfore will be negelected. The ground state hyperfine splitting for both isotopes of Rb are larger than 3 GHz, see table 2. The energy shifts due to the hyperfine splitting of ground state are given by:

$$\frac{\Delta E_F}{h} \quad = \quad \Delta\nu_F = \Delta x_F = \frac{A}{2}\left[F(F+1) - I(I+1) - \frac{3}{4}\right] \tag{76}$$

where I is the nuclear spin of the isotope and $F = I \pm \frac{1}{2}$.

This is large enough to worry about for Rb and therefore each line of Rb should be fit to a set of *four* Lorenztians, two for the hyperfine splitting and one for each isotope:

$$\begin{aligned} y \quad = \quad & 0.7217c_0\left(\frac{[1+0.664\times 2\pi c_1\,(x-c_2+1.264887)]}{(x-c_2+1.264887)^2+\frac{c_3^2}{4}} + \frac{[1+0.664\times 2\pi c_1\,(x-c_2-1.770844)]}{(x-c_2-1.770844)^2+\frac{c_3^2}{4}}\right) \\ & +0.2783c_0\left(\frac{[1+0.664\times 2\pi c_1\,(x-c_2+2.563005)]}{(x-c_2+2.563005)^2+\frac{c_3^2}{4}} + \frac{[1+0.664\times 2\pi c_1\,(x-c_2-4.271676)]}{(x-c_2-4.271676)^2+\frac{c_3^2}{4}}\right) \\ & +c_4 \end{aligned} \tag{77}$$

where x, the laser frequency, is in units of GHz.

Only one isotope of K has a hyperfine splitting of greater than 1 GHz. However, that isotope (^{40}K) is naturally abundant only at the ppm level, which is negligible. The more abundant isotopes of K have negligible (< 1 GHz) hyperfine splittings. The potassium D1 and D2 lines are very close (≈ 1700 GHz) compared to the expected widths (≈ 160 GHz). Note that this is not a problem for Rb, because the D1 and D2 lines are well separated (≈ 7100 GHz) compared to their widths (≈ 160 GHz). Although the D1 line for K and the D2 line for Rb are well separated (≈ 5000 GHz) compared to their widths (≈ 160 GHz), the relative size of the "peaks" is expected to be about 10 to 1 favoring K. This may mean that the K D1 line leaks into the Rb D2 line. We'll have to see what the data looks like, but if this is the case, then we'll need to fit the K D1, K D2, and Rb D2 lines altoghether. If that is not the case, then the Rb D2 can be fit separately but the K D1 and D2 lines still should be fit toghether (neglecting the small hyperfine splitting for K):

$$y \quad = \quad \underbrace{\frac{c_0\,[1+0.664\times 2\pi c_1\,(x-c_2)]}{(x-c_2)^2+\frac{c_3^2}{4}}}_{\text{D2}} + \underbrace{\frac{c_5\,[1+0.664\times 2\pi c_6\,(x-c_7-1730.32)]}{(x-c_7-1730.32)^2+\frac{c_8^2}{4}}}_{\text{D2}} + c_4 \tag{78}$$

4.5 Other Notes

In no particular order:

1. We took Burleigh data along with the Autoscan Wavemeter data. There appears to be an absolute shift in the frequency, however the scan is linear in frequency at better than the 0.5% level.

Iso.	$S_{1/2}$			$P_{1/2}$			$P_{3/2}$	
	A (MHz)	ν_{hfs} (MHz)	$x=1$ (gauss)	A (MHz)	ν_{hfs} (MHz)	$x=1$ (gauss)	A (MHz)	B (MHz)
^{6}Li	152.136 841	228.205 261	81.4	17.38	26.06	27.9	−1.155	−0.1
^{7}Li	401.752 043 3	803.504 086 6	287	45.92	91.83	98.4	−3.055	−0.22
^{23}Na	885.813 064 4	1 771.626 128	632	94.3	188.6	202	18.69	2.9
^{39}K	230.859 860 1	461.719 720 2	165	28.85	57.7	61.8	6.06	2.8
^{40}K	−285.731	−1 142.92	−405				−7.59	−3.5
^{41}K	127.006 935 2	254.013 870 4	90.6				3.40	3.3
^{85}Rb	1 011.910 813	3 035.732 439	1 080	120.72	362.16	388	25.01	25.88
^{87}Rb	3 417.341 306 4	6 834.682 612 8	2 440	406.2	812.4	870	84.845	12.52
^{133}Cs	2 298.157 942 5	9 192.631 770	3 280	291.9	1 167	1 250	50.34	−0.4
Ref.	AIV_{77}						AIV_{77}	

Table 2: Alkali atom ground State and first excited states hyperfine structure. AIV_{77} = Arimondo et al, RMP, 49, p31-75 (1977)

Isotope	**Mass** (amu)	**Natural Abundance**	**Nuclear Spin,** I	**Magnetic Moment** (μ_N)	**g-factor** $g_I(\mu_N)$
Lithium	6.941				
^{6}Li	6.015 122 3	0.075 9	1	+0.822 056	+0.822 056
^{7}Li	7.016 004 0	0.924 1	3/2	+3.256 44	+2.170 96
Sodium	22.989 770				
^{23}Na	22.989 769 7	1.0	3/2	+2.217 52	+1.478 35
Potassium	39.098 3				
^{39}K	38.963 706 9	0.932 58	3/2	+0.391 46	+0.260 97
^{40}K	39.963 998 7	0.000 117	4	−1.298	−0.324 5
^{41}K	40.961 826 0	0.067 30	3/2	+0.214 87	+0.143 25
Rubidium	85.467 8				
^{85}Rb	84.911 789	0.721 7	5/2	+1.353 02	+0.541 208
^{87}Rb	86.909 184	0.278 3	3/2	+2.751 2	+1.834 1
Cesium	132.905 45				
^{133}Cs	132.905 447	1.0	7/2	+2.579	+0.736 9
Reference	$NIST_d$		$NIST_e$		

Table 3: Alkali atom isotopic and nuclear data. $NIST_x$ = NIST websites

2. Since we have an absolute calibration of the Autoscan Wavemeter (from the Burliegh), we can in principle study the shifts in the lines as well.

3. Corney (forget the reference) has an equation that predicts the temperature dependance of the magic constant if the interaction potential is a power law. I forget what the formula is.

4. It would be interesting to see what the sign and order of magnitude of T_d for K is.

5 Things to do

1. Fill cells dedicated to a precise cross-calibration of magic constants.

2. Cell should have a relatively long path length and should have about a 1 to 1 ratio K to Rb at operating temperature.

3. We could fill four cells on a string with the same nominal mix of K to Rb, but with different pressures of buffer gas.

4. We would get the K D1 and D2 magic constants over a temperature range of 80C to maybe 200C for ^{3}He and N_2.

5. We would get the Rb D1 and D2 magic constants over a temperature range of 80C to maybe 200C for ^{3}He and N_2.

6. The Rb measurements at different temperatures for both ^{3}He and N_2 are necessary.

7. The Rb measurements at different buffer gas pressures is just a double check on our method.

8. The K measurements would probably be cross-calibrated with known precise values for Rb from Romalis et al.

9. As a bonus, we would gain more knowledge on how wel we can control the K to Rb by making many cells with a different nominal ratio.